International Journal of Pharmaceutics 704 (2026) 127399

Contents lists available at ScienceDirect

International Journal of Pharmaceutics

journal homepage: www.elsevier.com/locate/ijpharm

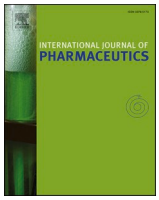

In vitro evaluation of water-insoluble silicates and polyvinylpyrrolidone-vinyl acetate as oral carriers for amorphous ritonavir: dissolution enhancement and the role of phosphatidylcholine

Gaurav Dhumal [a], Adélaïde Savoy [b], Martin Kuentz [b], James E. Polli [a,*]

[a] Department of Pharmaceutical Sciences, University of Maryland School of Pharmacy, Baltimore, MD, United States of America
[b] University of Applied Sciences and Arts Northwestern Switzerland, School of Life Sciences, Institute for Pharma Technology and Biotechnology, Muttenz, Switzerland

ARTICLE INFO

Keywords:
Silicate drug carriers
Ritonavir
Phosphatidylcholine
Aeroperl 300 pharma
Florite PS-200
High drug load
Molecular dynamics

ABSTRACT

Porous silicates have been investigated as drug carriers to promote the solubility and in vitro dissolution of poorly water-soluble drugs, owing to their potential to adsorb drug molecules in the amorphous form within their structural cavities. This study aimed to evaluate the efficiency of bentonite (BT), Aeroperl 300 Pharma (AP), and Florite PS-200 (FR) as water-insoluble silicate drug carriers, and the polymer polyvinylpyrrolidone-vinyl acetate (PVPVA) in improving the dissolution of ritonavir (RTV). The effect of phosphatidylcholine (PC) as a water-insoluble excipient on drug dissolution was also investigated. Multiple linear regression analysis of the dissolution data was performed to identify the factors influencing dissolution, complemented by mechanistic simulations of the best-performing carrier. The in vitro dissolution rank order of carriers with a 30% drug load (DL) based on % dissolved$_{300min}$ was AP = FR > PVPVA = BT in the absence of PC, and AP > FR > PVPVA > BT with PC. The extent of dissolution for all formulations increased in the presence of PC, with the AP and FR formulations exceeding that of marketed formulations. High drug load did not significantly affect the dissolution profile of silicate formulations, but it reduced dissolution from PVPVA solid dispersion. In silico results showed that silicate pore size governed RTV release, with open pores forming fewer hydrogen bonds, allowing more facile RTV release. The significant improvement in RTV dissolution with AP and FR supports the use of these carriers for poorly soluble drugs as alternatives to traditional polymers, especially for formulations with high drug loads.

1. Introduction

Many small-molecule drug candidates suffer from poor aqueous solubility, leading to an increased use of enabling technologies to mitigate this issue (Shah and Taylor, 2024). Amorphous solid dispersion (ASD) is an approach used to formulate Biopharmaceutical Classification System (BCS) Class II and Class IV drugs. Traditional binary ASDs consist of an amorphous drug molecularly dispersed in a polymer matrix, which acts as a crystallization inhibitor in the solid state and a supersaturation promoter in the liquid state (Bhujbal et al., 2021; Dhumal et al., 2024).

Water-insoluble drug carriers such as clays and silicas have recently been explored as alternatives to polymers to improve drug solubility and dissolution profiles. These silicate carriers are characterized by large surface areas owing to their porous structures. Drug molecules are both adsorbed on the surface and intercalated into the pores of the carrier to form a drug-carrier composite of amorphous drug (Van Speybroeck et al., 2010a). The confined pores prevent drug recrystallization (Bukara et al., 2016; Heikkilä et al., 2007; Van Speybroeck et al., 2010a). When the composite comes into contact with the buffer, the amorphous drug dissolves into the medium (Van Speybroeck et al., 2010b).

Common techniques for preparing drug-silicate composites are solvent impregnation and melt intercalation. Solvent impregnation involves dropwise addition of a drug solution (e.g., drug in methanol) to the drug carrier with continuous trituration until the solvent has evaporated. In this technique, the drug solution penetrates the carrier pores; upon solvent evaporation, the drug remains embedded in the pores in the amorphous state. Melt intercalation involves melting the drug in the presence of a carrier at a slightly higher temperature than the drug's melting point (Shen et al., 2002). It can be performed either by hot melt

* Corresponding author at: 20 Penn Street, Room 623, HSF2 Building, Baltimore, MD 21201, United States of America.
E-mail address: jpolli@rx.umaryland.edu (J.E. Polli).

https://doi.org/10.1016/j.ijpharm.2026.127399
Received 15 July 2026; Received in revised form 16 August 2026; Accepted 8 September 2026
Available online 8 September 2026

extrusion (HME) or vacuum compression molding (VCM) (Liu et al., 2020). It is solvent-free and scalable, but the drug must not be thermolabile. To the best of our knowledge, VCM has not been previously applied to prepare ternary drug-polymer-silica composites.

The findings of Baek et al. demonstrated that bentonite is a promising drug carrier to improve sorafenib solubility. In vivo rat studies showed that the sorafenib-bentonite composite increased bioavailability 3-fold relative to Nexavar (Baek et al., 2023). A similar study from the same group showed that the incorporation of PC boosted drug release from quetiapine-bentonite composites to address the partial drug release from bentonite (Baek et al., 2022). Dening and Taylor explored ordered mesoporous SBA-15 as a delivery vehicle for RTV (Dening and Taylor, 2018). The silica successfully maintained RTV in an amorphous form, but drug release was incomplete because of the adsorption equilibrium between silica and the dissolution medium. The presence of bile salts in the dissolution medium enhanced drug release from silica (Dening and Taylor, 2018). Bukara et al. conducted the first-in-human clinical study to evaluate the bioavailability-enhancing potential of mesoporous silica, with fenofibrate as a model drug. When normalized for dose, the fenofibrate-silica formulation showed a significant increase in the rate and extent of drug absorption as compared to Lipanthyl (Bukara et al., 2016).

Phosphatidylcholine (PC) is a phospholipid that is usually extracted from soybeans and egg yolk, but can also be produced synthetically. Owing to its surface-wetting and emulsifying/solubilizing properties, PC and other phospholipids have been used in drug delivery systems for poorly water-soluble drugs (Li et al., 2015). A study by Jo et al. involved the preparation of a PC-based dispersion using solvent evaporation to enhance celecoxib dissolution (Jo et al., 2019). PC alone enhanced celecoxib's solubility. However, due to the sticky nature of PC, the silica Neusilin US2 was used to convert the PC dispersion to a powdered form for oral solid administration. In a similar manner, Yeo et al. also incorporated silica to address the formulation's sticky behavior (Yeo et al., 2020).

Ritonavir was selected as the model compound because it is a good glass former. It is a weakly basic (pKa values of 1.8 and 2.6), poorly water-soluble drug typically used in combination with other antiviral drugs (Xu et al., 2018).

The primary goal of the current study was to evaluate the use of silicates as drug carriers to improve RTV's dissolution and to compare their overall dissolution performance with that of traditional RTV ASD made with the polymer PVPVA and with commercial formulations. It was hypothesized that, at high drug load, silica would provide higher drug dissolution than polymer since drug release from a non-dissolving carrier is not coupled to dissolution of the carrier itself.

Three chemically distinct water-insoluble carriers were selected to test this hypothesis across a deliberate gradient of surface area. Bentonite (BT), a naturally occurring clay/silicate, along with the synthetic silicas Aeroperl 300 Pharma (AP) and Florite PS-200 (FR), were selected as a silicate drug carriers. AP is a colloidal silicon dioxide, whereas FR is a calcium silicate. PVPVA was also studied as a traditional polymer to make RTV ASD formulations. Here, BT, AP, and FR are collectively referred to as silicates, and solvent impregnation was used to fabricate binary composites from these silicates. VCM was used to fabricate binary and ternary PVPVA ASDs in this study. BT, AP, FR and PVPVA are collectively referred to as 'carriers'. The impact of PC on the extent of dissolution of RTV formulations was also studied. Dissolution profiles of the formulations were compared to those of commercial RTV crushed tablets and powder. To identify the factors affecting dissolution, both positively and negatively, a multiple linear regression was carried out using dissolution data of binary formulations.

2. Materials and methods

2.1. Materials

Ritonavir was purchased from Chem Shuttle (Burlingame, CA, USA). Bentonite NF grade was obtained from Spectrum Chemical Mfg. Corp. (New Brunswick, NJ, USA). Aeroperl 300 Pharma was a gift from Evonik Industries AG (Essen, Germany). Florite PS-200 was generously donated by Tomita Pharmaceuticals Ltd. (Tokyo, Japan). PVPVA (Kollidon VA 64, copovidone) was obtained from BASF Corporation (Jessup, MD, USA). L-α-Phosphatidylcholine (Mol. Wt. = 790.15 g/mol) was purchased from Sigma-Aldrich (St. Louis, MO, USA). Aurobindo Ritonavir tablets (Aurobindo Pharma USA, NJ, USA), Packets of Norvir oral powder and Norvir Tablets (AbbVie; North Chicago, IL, USA) were commercially obtained. All other reagents were of analytical grade and obtained from Sigma-Aldrich (St. Louis, MO, USA).

2.2. Preparation of RTV-carrier composites

2.2.1. Solvent impregnation of AP, FR, and BT

To prepare formulations without PC, a concentrated RTV solution in methanol (25 mg/mL to 75 mg/mL) was added dropwise to an appropriate quantity of silicates to achieve 10%, 30%, and 50% drug loading. The mixture was stirred with a pestle until it appeared dry, then dried overnight under vacuum. It was gently crushed with a mortar and pestle and passed through a 75 μm sieve. Formulations were labeled by their carrier's name and 'No PC' (e.g., AP – No PC).

For formulations containing PC, 675 mg of PC was physically blended into the previously prepared formulations containing 27 mg of RTV. These formulations were labeled with the carrier name and '+ PC' (e.g., AP + PC). The PC:RTV weight ratio was 25:1 (i.e. 675 mg PC: 27 mg RTV) for all the PC-containing formulations. The ratio was selected for the present proof-of-concept study based on 675 mg PC being a potentially viable component of an oral dosage form, particularly compared to supplements in the United States that contain 1260 mg PC.

All composites were stored in a desiccator until further use. Composite drug content was confirmed using ultra-performance liquid chromatography (UPLC), as described below. Fig. 1 shows the formulation workflow for preparing both the binary and ternary formulations.

2.2.2. Melt intercalation with PVPVA and ternary ASDs

A physical mixture of RTV and PVPVA was prepared at 10%, 30%, and 50% drug loads using a cryo-mill. About 1 g of the blend was heated at 150 °C for 15 min in the MeltPrep VCM chamber (25 mm diameter) under vacuum, then immediately cooled for 5 min (MeltPrep GmbH, Graz, Austria) (Men and Polli, 2024). The resulting ASD discs were milled using a cryo-mill, sieved through a 75 μm sieve, and stored in a desiccator. Drug content was confirmed by UPLC as described below. To prepare RTV-PVPVA ASDs with PC, 675 mg of PC was physically blended with the cryo-milled ASD powder (containing 27 mg of RTV), similar to the binary silicate formulation.

Ternary ASDs containing RTV, PVPVA, and AP or FR in a 2:1:1 wt ratio were also prepared using VCM, following the steps described above. Two lacked PC, and two included PC. The ternary ASD of RTV, PVPVA, and AP was selected because RTV-AP exhibited the highest dissolution among binary formulations. The ternary ASD of RTV, PVPVA, and FR was selected because RTV-FR exhibited the second-highest dissolution among binary formulations. Fig. 2 shows the schematic illustration of the preparation of binary formulations using solvent impregnation and melt intercalation techniques.

2.3. Silicate tablet formulation

Based on the dissolution performance of binary silicates, AP performed the best as compared to FR and BT. Since drug loading had no significant impact on drug release, RTV-AP 10% DL was chosen to be

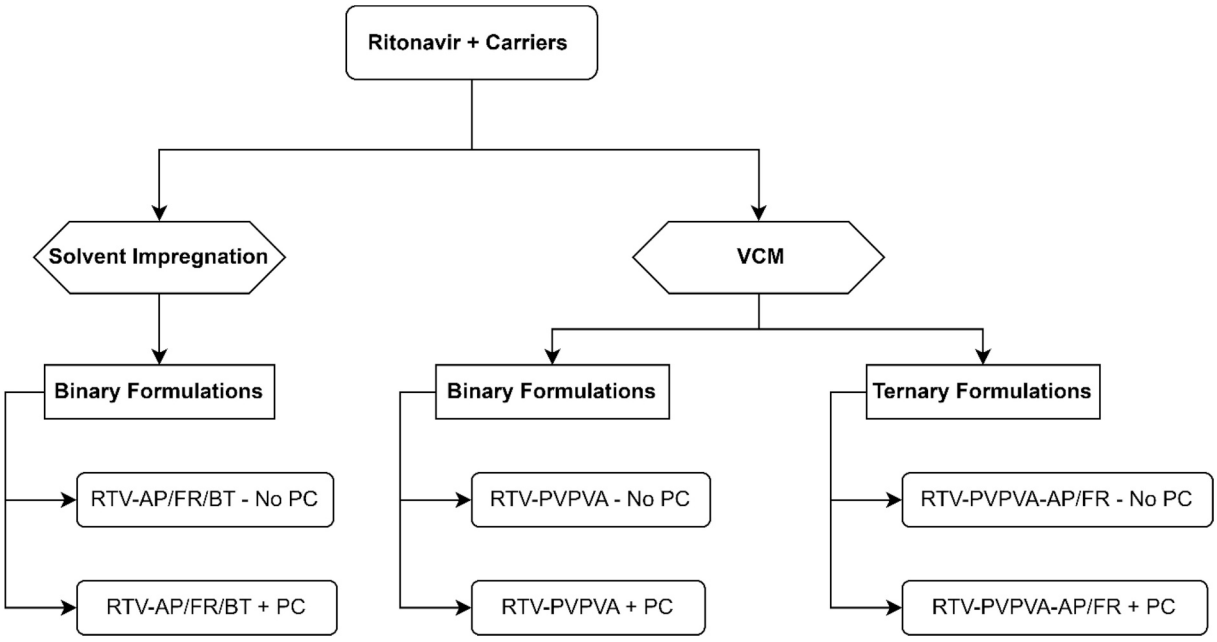

Fig. 1. Workflow for preparing binary and ternary ritonavir (RTV) formulations with and without phosphatidylcholine (PC). Solvent impregnation and vacuum compression molding (VCM) were employed to fabricate formulations.

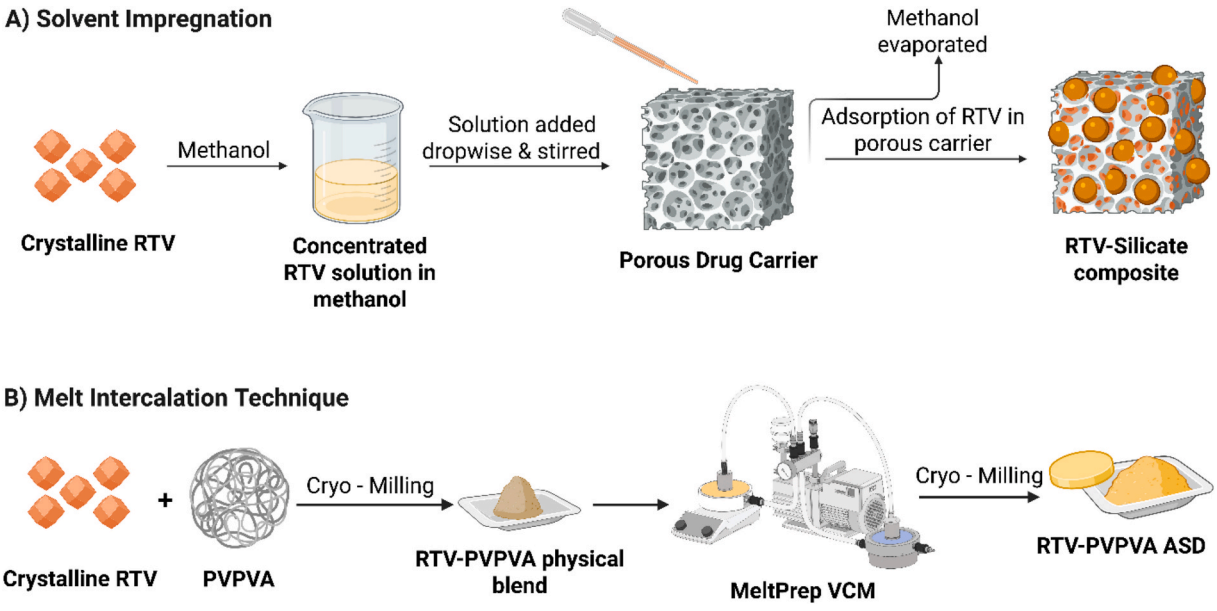

Fig. 2. Schematic illustration of the binary formulation preparation using solvent impregnation (Panel A) and melt intercalation technique (Panel B). Images are not drawn to scale.

tableted. Table S1 describes the tablet ingredients and their quantities. All ingredients except magnesium stearate were weighed and mixed using a Turbula Mixer for 5 min, followed by the addition of magnesium stearate and mixing for a further 2 min. A blend sufficient for 4 tablets was prepared fresh before tableting. A single-station Natoli NP-RD10A hydraulic press with a 10 mm diameter flat punch was used to fabricate tablets using a 500 N compaction force. Tablets were immediately subjected to in vitro dissolution (n = 3).

2.4. Ritonavir content quantification and ultra-performance liquid chromatography (UPLC)

The amount of RTV (%) in the dried formulations was determined by dispersing ~10 mg of composite/ASD powder in 2 mL of PBS (pH 6.8), then diluting 10-fold with methanol (final volume = 20 mL). The resulting suspension was sonicated for 30 min, vortexed for 30 min, and then centrifuged at 2000 × g for 15 min. The supernatant was filtered through a 0.45 μm polyvinylidene fluoride (PVDF) syringe filter, diluted with the mobile phase, and analyzed by UPLC. To calculate the % drug load (w/w) and % encapsulation efficiency in the composite/ASD, Eqs. (1) and (2) were used, respectively:

$$\%\,\text{Drug load (DL)} = \frac{\text{Amount of RTV in formulation (mg)}}{\text{Amount of formulation (mg)}} \text{ x } 100 \quad (1)$$

$$\%\,\text{Encapsulation efficiency} = \frac{\text{Measured drug load}}{\text{Theoretical drug load}} \text{ x } 100 \quad (2)$$

Ritonavir was quantified using a Waters Acquity H-Class UPLC system (Waters Corporation; Milford, MA) equipped with a photodiode array (PDA) detector. The mobile phase consisted of 0.05 M phosphoric acid and acetonitrile (53:47 v/v). An Agilent Zorbax SB-C18 column (5 μm, 4.6 × 150 mm) was used at room temperature. The flow rate was fixed at 1.0 mL/min, and the injection volume was 10 μL. The run time was 12 min, and the detection wavelength for RTV was set at 240 nm.

2.5. Equilibrium crystalline solubility

Excess crystalline drug was added to a scintillation vial containing 10 mL of potassium phosphate monobasic buffer (pH 6.8) and shaken at 37°C for 48 h. The samples were filtered through a 0.45 μm PVDF filter, and the pH of the filtrate was measured. The filtrates were diluted with the mobile phase and analyzed by UPLC. The experiment was repeated in triplicate (n = 3).

2.6. Characterization of RTV-carrier composites

2.6.1. Differential scanning calorimetry (DSC)

Crystalline ritonavir or the prepared RTV-composites/ASD was loaded into an aluminum T-zero pan and analyzed for crystallinity using a Discovery DSC 2500 (TA Instruments; New Castle, DE). The samples were heated to 150 °C at 10 °C/min, held isothermal for 5 min, cooled to 30 °C at 10 °C/min, held isothermal for 2 min, and finally reheated at 10 °C/min to 150 °C.

2.6.2. Particle size distribution

The particle size distribution of neat carriers was measured using a Malvern Mastersizer 2000 laser-diffraction particle-size analyzer with a Scirocco 2000 dry dispersion unit (Malvern Panalytical; Malvern, UK). The measurement time was set to 12 s. Each sample was measured in triplicate, and the mean and standard deviation values are reported.

2.6.3. True density

A helium pycnometer (AccuPyc 1330, Micromeritics, USA) was used to measure the true density of the neat carriers in triplicate. Values reported are the mean and standard deviation.

2.6.4. BET surface area

A Gemini VII surface area analyzer (Micromeritics, GA) was used to determine the specific surface area (SSA) of the neat silicate carriers and the prepared RTV composites. Samples weighing 0.3–0.5 g were degassed with nitrogen at 105°C for 2 h using the FlowPrep 060 unit (Micromeritics, GA). Adsorption measurements were recorded at relative pressures from 0.05P/Po to 0.3P/Po. Brunauer–Emmett–Teller (BET) SSA calculations were performed using the Gemini VII software (version 5.0.1).

2.6.5. Stability testing

Formulations without PC at various drug loads were evaluated for amorphous stability by storing the samples in a sealed aluminum bag under accelerated conditions (40 °C/75% RH) for 30 days. The samples were then analyzed by DSC to assess crystallinity, following the protocol described above.

2.6.6. Attenuated total reflectance-Fourier transform infrared spectroscopy (ATR-FTIR)

The molecular-level interaction between RTV and clay/silica carriers and PVPVA was studied using spectroscopic analysis. Spectra of the samples were recorded on a Jasco FTIR-6100 (Jasco Analytical Instruments; Easton, Maryland) from 400 to 4000 cm^{-1} with a resolution of 4 cm^{-1}. For each spectrum, 64 scans were collected and averaged.

2.7. In vitro dissolution

In vitro dissolution of 28 RTV formulations (with and without PC), along with unformulated drug and unformulated drug with PC, was performed. Unformulated drug with PC was prepared by physically mixing the drug with PC at a 25-fold weight ratio of PC to drug.

Dissolution was performed in a USP Type-II apparatus using 900 mL of 50 mM potassium phosphate monobasic buffer (pH 6.8) maintained at 37 ± 0.5 °C, with a paddle speed of 100 rpm. An amount of each formulation equivalent to 27 mg of RTV was added to each vessel, corresponding to the amorphous solubility of RTV (30 μg/mL) (Men and Polli, 2024). For PC-containing formulations, this addition introduced 675 mg of PC into 900 mL of buffer, yielding a PC concentration of 0.95 mM, which is lower than the lecithin content (primarily PC) in FeSSIF (3.75 mM) and FeSSIF-V2 (2 mM) (Roger et al., 2009).

Samples (2 mL) were withdrawn at 10, 20, 30, 45, 60, 90, 120, 150, 180, 240, 300, and 330 min using a syringe with a 21G × 2″ TW needle. After 300 min, the paddle speed was increased to 250 rpm, and a sample was collected at 330 min (i.e., infinity spin). For each sample, the needle was immediately replaced with a 0.45 μm syringe filter. The first 1 mL was discarded, and the remaining 1 mL was collected. The filtrate was immediately diluted with the mobile phase and analyzed by UPLC.

Fabricated tablets of RTV-AP-10% DL (27 mg RTV per tablet) were subjected to dissolution procedure as mentioned above. Commercial products of RTV, i.e., Norvir tablets, Norvir powder, and generic ritonavir tablets from Aurobindo, were also subjected to in vitro dissolution. Norvir tablets and Aurobindo tablets were cryo-milled to a powder before dissolution, whereas Norvir powder was used as received. Dissolution was performed as described above (i.e., the amount of formulation containing 27 mg of RTV was added to each vessel). All dissolution experiments were repeated in triplicate (n = 3), and the average was plotted with the standard error of the mean (SEM).

In vitro biorelevant dissolution was also performed in FaSSIF-V2 medium (100 mL) for RTV-AP-50% and Norvir Powder, at 3 mg RTV equivalent dose and 100 rpm paddle speed. The buffer-medium-to-dose ratio was the same as that used for the phosphate buffer dissolution. Sampling was similar to that described previously.

2.8. Statistical modeling

Dissolution data of binary formulations were analyzed using multiple linear regression (standard least squares) with backward elimination in JMP software version 19 (SAS Institute; Cary, NC, USA). The model evaluated the effects of the main factors (i.e., carrier type, drug load, and the presence/absence of phosphatidylcholine) and their second-order interactions on the percent of drug dissolved at 5 h. The Akaike Information Criterion (AIC) was used to select the best model. Standard regression diagnostics, including R^2, root mean square error (RMSE), and parameter statistical significance (p-value < 0.05), were used to assess model performance. In backward elimination, the least significant term was removed from the model until the AIC value increased.

2.9. Molecular dynamics simulations

In-silico investigations of the ritonavir-silica pore system were undertaken using classical molecular dynamics (MD) simulations. The silica pore with a 4 nm diameter was generated by connecting silicon and oxygen atoms, whose positions had been generated using the PoreMS script (Kraus et al., 2021). The outer surfaces with pore openings (front and back) bore trimethylsilyl (TMS) groups, which was a surface modification for the simulation aimed at trapping the RTV upon release. This was designed to avoid the artificial re-entry of RTV into the pores owing to the periodic boundary condition used during the simulations. The overall pore structure was approximately 6 × 6 × 10 nm. The MD simulations were carried out using the Maestro software (version 14.3) by Schrödinger (release 2025-2) with the OPLS4 (Lu et al., 2021) force

field.

The workflow for the MD simulation is illustrated in Fig. 3. The most stable conformer of ritonavir in vacuum was calculated with MacroModel (Mohamadi et al., 1990) as implemented in Maestro and was inserted in the middle of the pore. All subsequent simulations were done in triplicate with different random seeds. After energy minimization using the material relaxation protocol, as implemented in Maestro, the 25 ns NPT production runs in the gas-phase were simulated at 300 K and 1.01 bar. The boxes for the aqueous simulations in the closed pore were prepared by generating a 10 × 10 × 12 nm box surrounding the pore + RTV system, using the geometry from the last frame of each of the three gas-phase simulations. For the simulations in the open pore, the geometry of the last frame of the gas-phase simulation was altered before the box generation: half of the pore was removed through a vertical cut. Additionally, the sharp edges resulting from the cut were truncated. The two sets of triplicate (closed and open pore) were then simulated using a workflow adapted from the literature (Skrdla et al., 2023), which consisted of the material relaxation protocol, followed by a 10 ns NPT equilibration (1.01 bar, 298.1 K) with subsequent box resizing based on the average volume over the last 20% of the equilibration trajectory. The production run was a 250 ns NVT simulation at 298.0 K. The intermolecular non-aromatic hydrogen bonds between the ritonavir molecule and the silica pore were monitored over the trajectory using the interaction tool built into the Maestro software.

3. Results and discussion

3.1. Preparation of RTV-carrier formulations

Ritonavir formulations with varying drug loads were prepared using solvent impregnation and VCM. The drug content and encapsulation efficiency of each formulation are summarized in Table S2. All formulations had an encapsulation efficiency of 80% or higher.

3.2. Physical properties of neat carriers

The physical properties of drug carriers determine drug-carrier/polymer interactions and subsequent drug dissolution. Common physical properties, including SSA, particle size distribution, and true density of the neat carriers, are listed in Table 1. AP exhibited the highest SSA (255.54 ± 3.53 m^2/g), whereas BT showed the lowest (16.36 ± 0.02 m^2/g), despite similar particle size distributions. Thus, the differences in surface area among all silicates reflected structural features rather than particle size alone.

Table 1
Physical properties of neat drug carriers. AP, FR, and BT are silicates whereas PVPVA is a polymer. (mean ± SD).

		Aeroperl 300 Pharma (AP)	Florite PS-200 (FR)	Bentonite (BT)	PVPVA
Common name		Colloidal silicon dioxide	Calcium Silicate	Montmorillonite (major component)	Copovidone
Specific surface area (m^2/g)		255.54 ± 3.53	155.93 ± 1.56	16.36 ± 0.02	–
Particle Size (μm)	d10	2.59 ± 0.09	5.02 ± 0.01	3.62 ± 0.05	14.11 ± 0.03
	d50	10.75 ± 1.17	18.17 ± 0.14	12.48 ± 0.22	45.04 ± 0.08
	d90	30.49 ± 2.38	102.14 ± 1.93	31.11 ± 1.12	110.64 ± 0.43
True density (g/cm^3)		2.3 ± 0.03	2.5 ± 0.05	2.5 ± 0.004	1.2 ± 0.01

3.3. Differential scanning calorimetry

The DSC thermograms of crystalline RTV and the 14 formulations without PC are shown in Fig. 4. Crystalline RTV exhibited a sharp endothermic peak at 124.3 °C, corresponding to its melting point. In contrast, binary and ternary formulations containing BT, AP, FR, and/or PVPVA showed no endothermic peak. Thus, RTV was predominantly non-crystalline within the detection capability of the method. Similarly, analysis of stability samples showed that the drug remained amorphous throughout the stability period of 30 days at 40 °C/75% RH, as no melting endothermic peak was observed (Fig. S1). In formulations with silicates, this amorphization was attributed to the confinement of the drug within the pore space of the silica matrices, which restricted molecular mobility and prevented drug recrystallization during 30 days of storage at 40 °C/75% RH.

3.4. BET specific surface area

The specific surface areas (SSAs) of neat drug carriers and their RTV-

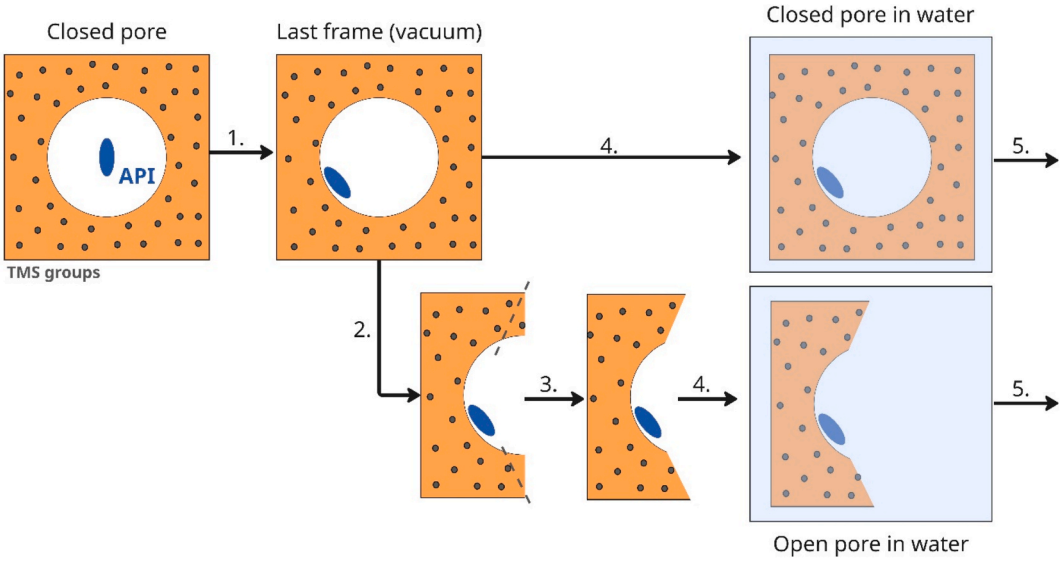

Fig. 3. Workflow for the preparation of the MD simulations. 1) 25 ns simulation in vacuum. 2) Deletion of half of the pore. 3) Truncation of the sharp interior edges. 4) Preparation of a 10 × 10 × 12 nm box of water with the pore + ritonavir system. 5) Simulation in water.

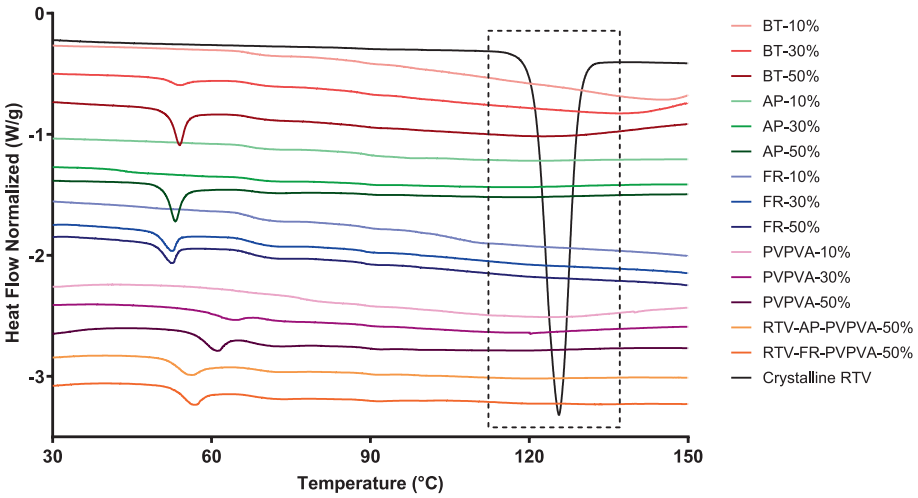

Fig. 4. Differential scanning calorimetry thermograms of crystalline RTV and 14 freshly prepared formulations without PC. There were four different carriers and three different drug loads. Two formulations contained three components (i.e., RTV at 50% DL, PVPVA, and either AP or FR).

composite formulations were measured to assess how drug loading affected SSA. Results are summarized in Table 2. SSA decreased consistently across all three carriers, with higher drug loadings yielding lower SSA. As more drug was deposited in carrier pores, less surface area was measurable. Although drug deposition reduced SSA across all loadings, the magnitude of the reduction was carrier-dependent, with bentonite showing the most pronounced decrease, while AP retained the highest SSA even at 50% DL. Formulations containing PVPVA could not be analyzed because the polymer and its formulations softened at 105°C.

3.5. Fourier transform infrared spectroscopy (ATR-FTIR)

FTIR spectroscopy was employed to evaluate the solid-state properties and potential intermolecular interactions between RTV and silicas/polymer in binary and ternary formulations (Fig. 5). Crystalline RTV showed a sharp N–H stretch at 3324 cm^{-1} and three sharp peaks representing carbamate (1702 cm^{-1}), ureido (1660 cm^{-1}) and amide (1609 cm^{-1}). In contrast, amorphous RTV exhibited a broadened N–H region centered near 3290 cm^{-1} along with a broadened amide-ureido merged band at 1626 cm^{-1}.

For all RTV-silica composites with 50% DL, the sharp triplet peaks seen in crystalline RTV were replaced by broad N–H envelope and merged carbonyl band (1630 cm^{-1}). The RTV carbonyl shifted slightly upward from 1626 cm^{-1} to 1628 cm^{-1}, 1631 cm^{-1}, and 1632 cm^{-1} for RTV-BT, RTV-AP, and RTV-FR, respectively. This small displacement across all silica formulations indicates partial disruption of RTV–RTV interactions and relocation of the drug onto surface hydroxyls of silicas. The distinct bands of silica framework remained unchanged, pointing towards surface–level interactions only.

In the case of the RTV-PVPVA binary ASD (50% DL), the polymer carbonyl at ≈1673 cm^{-1} was a dominant feature and showed no shift, whereas the N–H stretching region of RTV appeared as an increasingly pronounced and broadened band, reaching 3307 cm^{-1}, shifted by +17 cm^{-1} relative to neat amorphous RTV. Additionally, the characteristic drug bands at 1626 cm^{-1} was no longer resolved. These changes indicate loss of RTV self-association and molecular-level mixing with the polymer. The absence of a red shift or low–wavenumber shoulder in the pyrrolidone carbonyl shows that only limited polymer carbonyls engage in hydrogen bonding with RTV, and incorporation of silica did not alter this interaction

Ternary cryo-milled ASDs of RTV with PVPVA and either Aeroperl or Florite (2:1:1, 50% DL) also showed complete disappearance of crystalline RTV markers. Instead, the spectra were dominated by the broad N–H stretching region of amorphous RTV (~3280–3300 cm^{-1}). These observations further confirmed that RTV remained molecularly dispersed in an amorphous state within the ternary matrices.

Table 2
Specific surface areas of RTV-silicate composites. For reference, SSAs of neat carriers were 16.36 ± 0.02 m^2/g for BT, 255.54 ± 3.53 m^2/g for AP, and 155.93 ± 1.56 m^2/g for FR. (mean ± SD).

Samples	Specific Surface Area (m^2/g)
RTV-BT 10% DL	5.67 ± 0.03
RTV-BT 30% DL	1.31 ± 0.01
RTV-BT 50% DL	0.14 ± 0.01
RTV-AP 10% DL	165.76 ± 1.11
RTV-AP 30% DL	92.21 ± 0.64
RTV-AP 50% DL	33.06 ± 0.22
RTV-FR 10% DL	116.33 ± 0.80
RTV-FR 30% DL	75.13 ± 0.49
RTV-FR 50% DL	28.90 ± 0.21

3.6. In vitro dissolution

3.6.1. Main effects

The in vitro powder dissolution profiles of all 28 formulations (including those with and without PC), along with the unformulated drug, are shown in Figs. 6 and 7. The figures differ in drug load. The paddle speed was 250 rpm between 300 and 330 min. All formulations exhibited markedly higher drug release than the unformulated crystalline RTV, which had an equilibrium solubility of 0.0013 mg/mL. Drug load did not reduce dissolution in silicate formulations, unlike PVPVA, for which dissolution decreased with higher drug load. This difference represents the single largest advantage of silicates over the polymer PVPVA.

In the absence of PC, the formulations reached 30–45% dissolution before plateauing. RTV-PVPVA 10% DL (both with and without PC) showed immediate release of drug, whereas the silicate counterparts showed more gradual release (Fig. 6). The incorporation of PC significantly enhanced drug release across all formulations, yielding substantially greater dissolution than without PC. The presence of PC only minimally enhanced the dissolution of the unformulated drug. The increased drug release from silicate and PVPVA formulations was attributed to improved wettability. Based on the % $dissolved_{300min}$, the rank order obtained for the carriers at 30% DL was AP = FR > PVPVA = BT in the absence of PC, and AP > FR > PVPVA > BT with PC.

The effect of drug loading depended on the carrier type. Increasing drug loading reduced dissolution from PVPVA, whereas the dissolution performance of the silicate formulations was comparatively insensitive

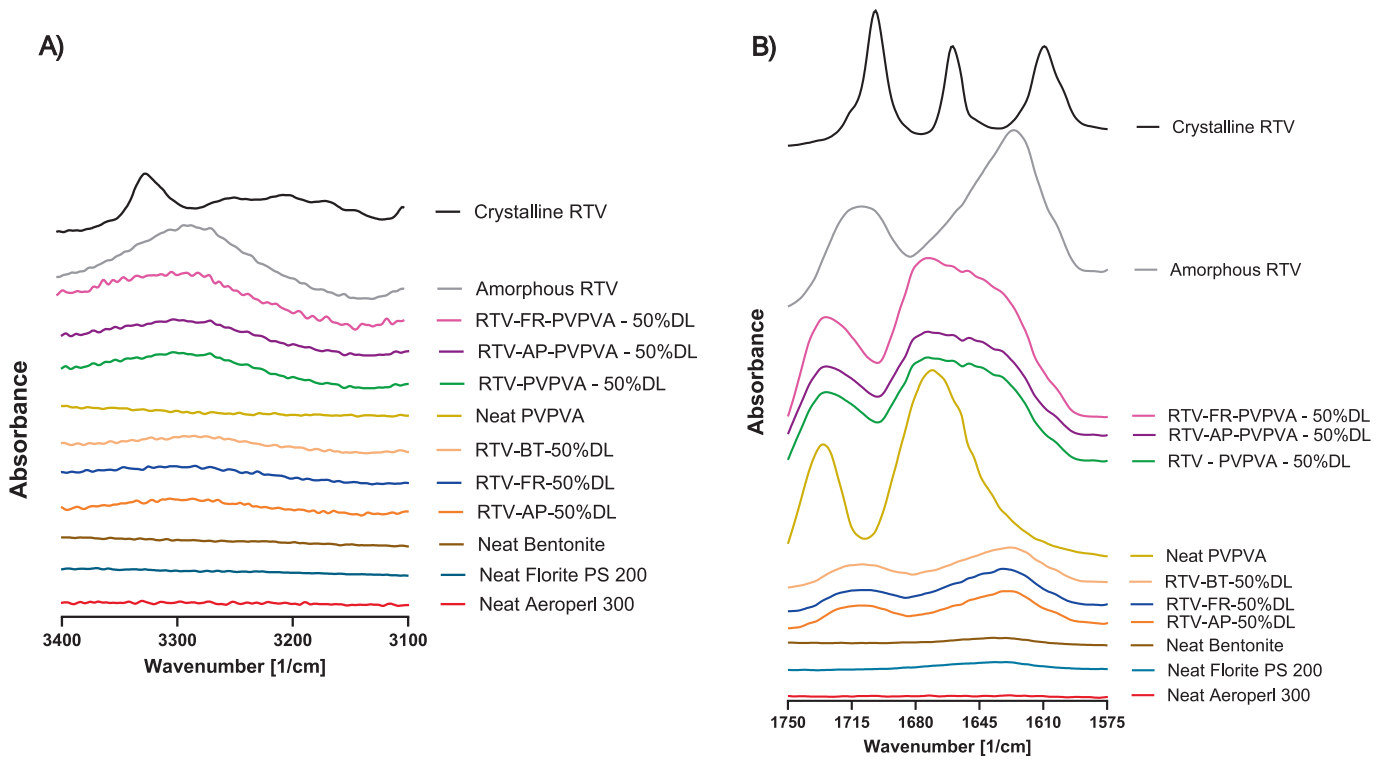

Fig. 5. FTIR spectra of neat components and binary and ternary formulations containing 50% DL. Panel A shows the spectra from 3100 cm^{-1} to 3400 cm^{-1}, while Panel B shows the spectra from 1575 cm^{-1} to 1750 cm^{-1}.

to drug loading over the investigated range. BET analysis demonstrated progressive occupation of the silicate surface, as the specific surface area decreased with increasing drug loading. Nevertheless, AP and FR retained specific surface areas of 33.06 ± 0.22 and 28.90 ± 0.21 m^2/g, respectively, at 50% drug loading. The remaining accessible surface area and pore structure may therefore have been sufficient to permit water penetration and release of amorphous RTV over the loading range investigated. Therefore, the experiment showed that a smaller amount of silicate was still sufficient to carry the same 27 mg drug dose without substantially reducing dissolution.

A limitation of this study is that drug loads above 50% were not evaluated. Therefore, the observed dissolution behavior should not be assumed to apply beyond the drug-loading range investigated in this study.

When comparing ternary ASD formulations (50% DL) with their 50% DL binary counterparts without PVPVA, the effect of added PVPVA depended on the silicate (Fig. 7). The addition of PVPVA to the AP-containing ASD had no effect on the dissolution. The RTV-AP-PVPVA ASD dissolution profile was similar to RTV-AP; the same was observed for the ASD with PC. By contrast, the addition of PVPVA to the FR-containing ASD had a detrimental effect, such that the dissolution of the RTV-FR-PVPVA ASD was similar to that of RTV-PVPVA; the same was observed for the ASD with PC. Thus, for the FR-containing ternary system, the retarding effect of PVPVA remained dominant, and the inclusion of FR did not meaningfully alter drug release. Conversely, AP in the ternary system was able to counteract PVPVA's tendency to reduce dissolution at high drug loading, resulting in improved performance.

Of note, no dissolution profile reached 100% dissolved, which would require all 27 mg of drug to dissolve in the 900 mL volume, attaining the amorphous solubility of RTV (30 μg/mL). Rather, the highest percent dissolved was 86.4% from RTV-PVPVA-10% DL with PC, and the second highest was 70.3% from RTV-AP 30% DL with PC (Fig. 6, Panel B). Non-sink conditions were a reason for incomplete release within 5 h in phosphate buffer, although most profiles tended to show a nearly flat plateau, suggesting a thermodynamic barrier to further release. Other studies of silicates also showed incomplete release with flat profiles (Baek et al., 2022, Baek et al., 2023, Dening and Taylor, 2018).

3.6.2. *Comparison to commercial products*

Dissolution testing was also performed on three commercial ritonavir products: Norvir powder, the Norvir tablet, and the generic ritonavir tablet from Aurobindo. The crushed Norvir tablet released approximately 45% of the drug within 45 min; the amount then declined progressively, reaching about 25% at 330 min (Fig. S2). Norvir powder reached a plateau after releasing 30% and did not decline over time. The crushed Aurobindo tablet showed the lowest release, with an initial release near 35% that declined over time, reaching 20% at 330 min. Release profiles were incomplete.

Overall, the RTV-AP formulations with 10% and 30% DL (without PC) showed drug release comparable to that of Norvir powder. Dissolution profiles of RTV-PVPVA 10% DL ASD (without PC) were similar to those of the Norvir tablet. It should be noted that both Norvir powder and Norvir tablet contain sorbitan monolaurate as a surfactant in their formulations. Although the silicate-based formulations showed a slower initial release rate, they sustained drug supersaturation throughout the dissolution testing period. Furthermore, incorporating PC enhanced dissolution beyond the extent observed in the commercial formulations.

In FaSSIF–V2, the commercially formulated Norvir powder (15% DL with PVPVA and sorbitan monolaurate as a surfactant; Ellenberger et al., 2018) exhibited a pronounced burst release, delivering approximately 80% of RTV within the first 20 min. In contrast, the RTV–AP 50% DL formulation displayed a more controlled and sustained release profile, achieving 80% drug release only after approximately 5 h (Fig. 8). Interestingly, only ~6 mg of RTV-AP-50% DL was needed for the dissolution, whereas ~21 mg of the total Norvir powder sachet was required.

Dissolution parameters such as C_{max}, T_{max}, maximum degree of supersaturation and concentration decline at the end of 5 h dissolution are shown in Table S3.

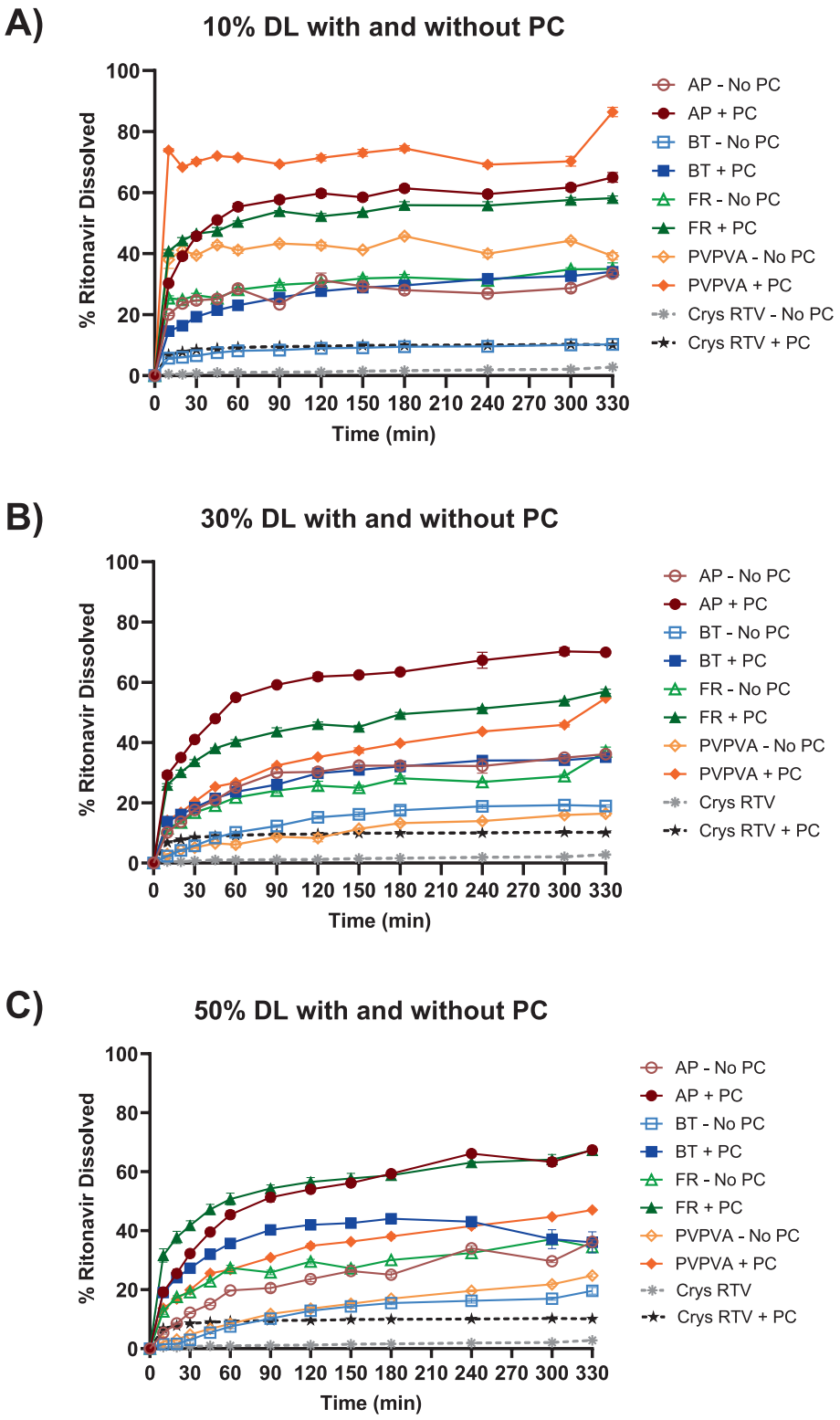

Fig. 6. In vitro dissolution profiles of binary RTV formulations containing drug and either silicate or PVPVA in phosphate buffer. Panels A, B, and C show the eight RTV formulations with 10%, 30%, and 50% DL, respectively. The eight formulations differed in carrier and in the presence or absence of PC. Also plotted are profiles from crystalline RTV and crystalline RTV with PC. Error bars are not drawn when too small to view.

3.6.3. Silicate tablet

In Fig. S3, the silicate tablet showed a slower release rate than the neat composite powder, owing to disintegration-dependent release (Li et al., 2023). This slow dissolution was due to the reduced tablet surface area exposed to the buffer, compared with that of the powder. The powder composite showed an initial burst release followed by plateauing, whereas the tablet showed a slow release. This was not an advantage here because rapid dissolution from powder did not result in drug precipitation, as tablets with slow drug release can avoid drug precipitation (Coutinho et al., 2025).

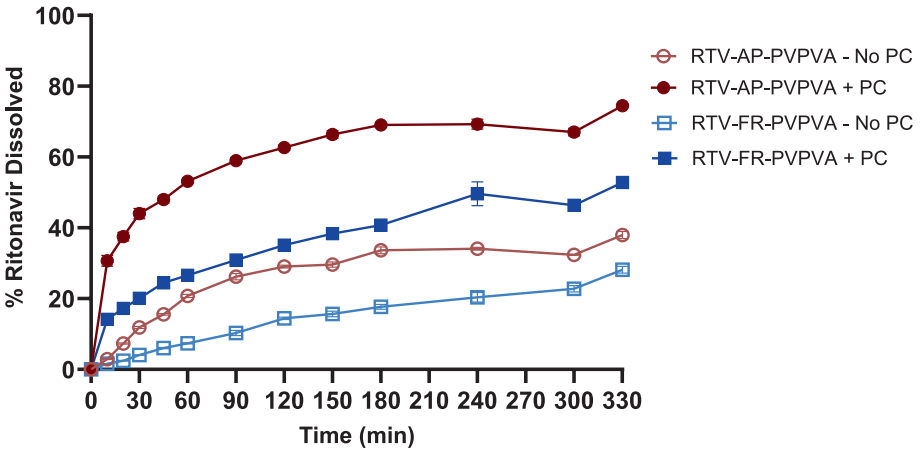

Fig. 7. In vitro dissolution profiles of four ternary RTV formulations with drug, silicates, and PVPVA in phosphate buffer. The four formulations differed in the type of silicate (i.e., AP or FR) and the presence or absence of PC. Drug load was 50%. Error bars are not drawn when too small to view.

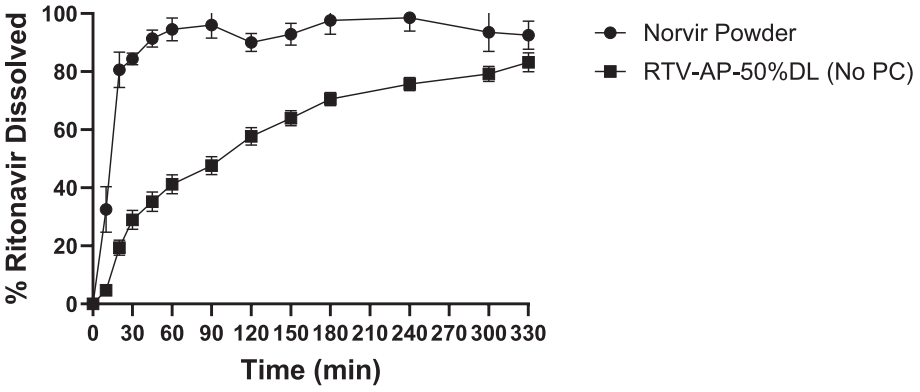

Fig. 8. In vitro dissolution profiles of commercial Norvir powder (15% DL) and RTV-AP-50% DL in FaSSIF-V2 buffer.

3.7. Statistical Modeling

Using backward elimination, a multiple linear regression model was identified to evaluate the effects of the factors, specifically the type of carrier (nominal), presence/absence of PC (ordinal), drug load (continuous), and their two-way interactions on the percentage RTV dissolved at 5 h. The initial model, containing all main effects and two-way interaction terms, had an AIC of 212.76, RMSE = 6.35, and R^2 = 0.94. The final model had an AIC of 178.13, RMSE = 6.37, and R^2 = 0.91. Further removing the next least significant term, the 'carrier × drug load' interaction, from the final model would result in an AIC of 179.68, RMSE = 8.07, and R^2 = 0.83; consequently, the AIC and RMSE increased, and the R^2 decreased.

The final model included the main effects of PC ($p < 0.0001$) and carrier ($p < 0.0001$), as well as a 'carrier × drug load' interaction ($p = 0.01$). Table 3 lists the parameter estimates, with carrier treated as a nominal factor using reference-level parameterization, PVPVA as the reference. Statistically significant terms that favored dissolution, relative to the intercept value of 26.9% dissolved, were PC, AP, and FR. The presence of PC produced a significant improvement in dissolution, regardless of carrier or drug load. In the model, carriers AP, FR, and BT were evaluated relative to PVPVA performance, and none of their interaction effects with drug load were statistically significant. The scaled estimates are shown in Table S4.

Table 3
Parameter estimates from multiple linear regression of percent RTV dissolved at 5 h. The regression included main effects (i.e., four carrier types, three drug loads, and presence/absence of phosphatidylcholine) and their second-order interactions. Carrier type was nominal. Drug load (i.e., 10%, 30%, and 50%) was treated as continuous. PC was treated as ordinal, with encoding of 1 for present and 0 for absent.

Term	Estimate	Std Error	t Ratio	Prob>|t|
Intercept	26.855833	1.839584	14.60	<0.0001*
Carrier[AP]	8.1820833	2.253021	3.63	0.0022*
Carrier[BT]	−14.88958	2.253021	−6.61	<0.0001*
Carrier[FR]	6.15375	2.253021	2.73	0.0148*
PC[1–0]	26.110833	2.601564	10.04	<0.0001*
Carrier[AP]*(% DL-30)	0.11125	0.137969	0.81	0.4319
Carrier[BT]*(% DL-30)	0.2205	0.137969	1.60	0.1296
Carrier[FR]*(% DL-30)	0.188875	0.137969	1.37	0.1899

3.8. Computational investigation of selected carrier and confinement

The carrier with the best release performance, Aeroperl 300 Pharma (AP), is a mesoporous silica material. To gain insights into the interactions between the RTV and this carrier, MD simulations of RTV in silica pores were undertaken. The number of non-aromatic hydrogen bonds was monitored over the trajectories of each simulation, and its average (Fig. 9) served as a qualitative measure of the interaction frequency and strength.

The simulation workflow is illustrated in Fig. 3. The first system was a single molecule of ritonavir in a mesoporous (4 nm) silica pore, referred to here as "closed pore", with TMS-substituted outer front and back surfaces. This hydrophobic layer was meant as an artificial trap, where the lipophilic API was expected to adsorb upon exiting the pore (Vraníková et al., 2020). Owing to the periodic boundary conditions, the

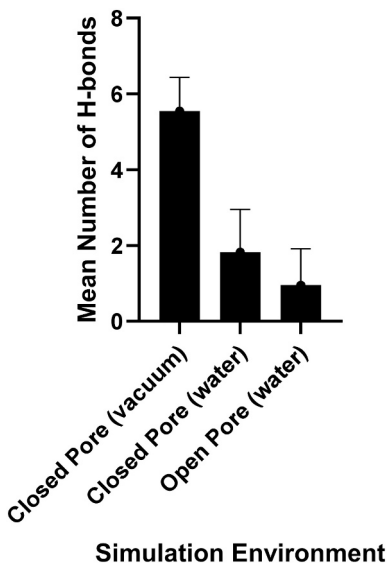

Fig. 9. Average number of ritonavir-pore non-aromatic hydrogen bonds per frame. Averaged over the trajectory of the three replicates.

API would likely re-enter the silica pore, which does not reflect the experimental conditions. Trapping API molecules that exited the pore avoids this artifact, and any RTV molecule sticking to the hydrophobic surface was considered "released into the bulk".

The closed pore was first simulated in vacuum to study non-covalent interactions between the pore and the RTV under conditions similar to a post-loading environment, although neglecting possible drug-drug interactions. Due to the lack of solvent, there was no attenuation of the non-covalent interactions between the silica pore and RTV, which was consistent with the high average number of hydrogen bonds per frame (5.5 ± 0.9). The mobility of RTV in the simulated pore was highly restricted, likely due to the multiple API-pore hydrogen bonds.

This was no longer the case in the presence of water, as the presence of a solvent attenuates the strength of non-covalent interactions (Pollice et al., 2017; Liu et al., 2025). Additionally, water molecules can also compete with the RTV-silanol hydrogen bonds. The presence of solvent resulted in a significantly lower average number of hydrogen bonds per frame (1.8 ± 1.1) between RTV and silica. In water, RTV moved within the pore by gliding on the pore surface, by anchoring through hydrogen bonding at a different point of the pore (Fig. 10), or by dissociating and subsequently re-attaching. Over all three trajectories, RTV did not drift far enough to exit the pore.

Displacement through anchoring or re-attachment would statistically be less likely to occur in a less confined environment. The simulated pore reflected a mesoporous silica with a relatively lower pore size, whereas the relatively larger pore size (30 nm) of the Aeroperl 300 material (Vraníková et al., 2020) would call for a less confined pore to mimic the experimental conditions more adequately. To examine if a less confined environment would provide more release, "open pores" were prepared and simulated in water (Fig. 3).

The number of non-aromatic hydrogen bonds was, on average, lower in the open than in the closed pore (0.6 ± 1.0). This lower average can be explained by the prolonged periods during which RTV was dissociated from the inner surface or was trapped outside of the pore. RTV showed qualitatively higher mobility through the box than in the closed pore system. All trajectories ultimately resulted in the exit of RTV from the pore, characterized by the RTV molecule sticking to the TMS-substituted hydrophobic layer (Fig. 11).

This ease of release from the open pore was consistent with the experimental observations, where RTV showed an enhanced dissolution performance when loaded onto AP, a silicate carrier with a 30 nm pore. Based on these observations, the release of RTV from silica pores appears to depend on the confinement within the pore. This conclusion was likely influenced by the structure of RTV. A drug with weaker API-silicate interactions may not exhibit the same confinement dependence of release performance. The caveat of calculations with a single drug molecule is that all drug-drug interactions, potentially leading to crystallization or aggregation, are overlooked. For molecules that tend to recrystallize, which is of lesser relevance for a good glass-forming drug such as ritonavir, smaller pores might be required for physical stability (Vraníková et al., 2020), despite a possible trade-off in release extent and speed.

Mesoporous carriers are often considered specifically suited for formulating poor glass-forming drugs that challenge conventional polymer-based solid dispersions (Ditzinger et al., 2019). However, the present study demonstrates that even in the case of a good glass-forming drug such as RTV, mesoporous carriers can be clearly advantageous regarding drug release at a higher drug load compared with polymer-based amorphous dispersions. Due to the nature of such drugs, relatively larger pore-sized materials can be selected to support a high drug release. Having comparatively less confined drug would be advantageous in the case of strong molecular drug-carrier interactions such as those observed for RTV and silica because it would not compromise drug release. It may additionally support the loading process and physical stability on storage, but these mechanistic conjectures based on the in-silico results were beyond the experimental scope of the present study.

4. Conclusion

The water-insoluble silicate carriers Aeroperl 300 Pharma (AP),

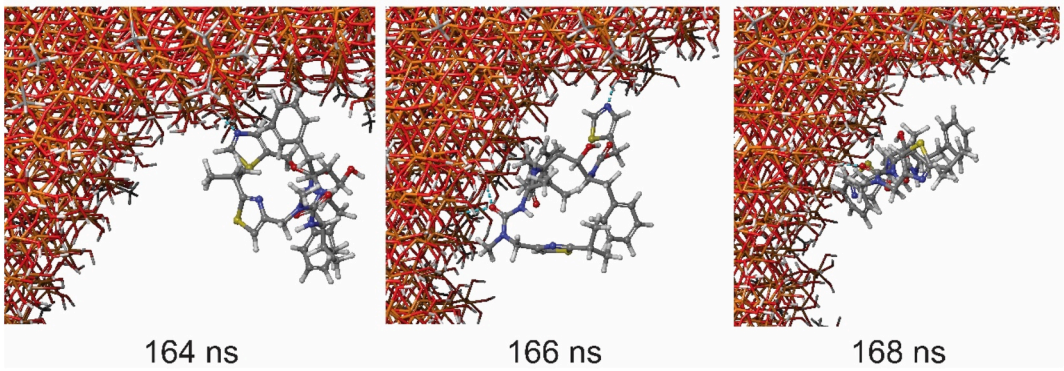

Fig. 10. Snapshots of the closed pore simulation in water. Simulations show the movement of ritonavir molecules from one side of silica pore to the other during hydrogen bond anchoring. The time since the start of simulation in ns is indicated under each snapshot. For clarity, the solvent molecules are not displayed. Non-aromatic hydrogen bonds are represented by a light blue dashed line.

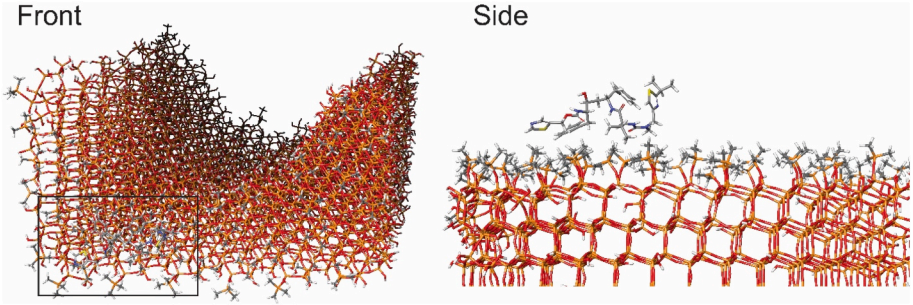

Fig. 11. Section of the last frame from the open pore simulation in water. RTV interacts with the TMS group on the modified outer front surface of the pore. Once adsorbed on the lipophilic surface, the ritonavir molecule is considered released from the simulated pore. For clarity, the solvent molecules are not displayed.

Florite PS 200 (FR), and bentonite (BT), and the water-soluble polymer polyvinylpyrrolidone-vinyl acetate (PVPVA) were evaluated for their ability to enhance RTV dissolution. Formulations of the four carriers were prepared using solvent impregnation and melt intercalation techniques. AP and FR showed greater dissolution enhancement than BT across all drug loads. In contrast, PVPVA exhibited drug-load-dependent dissolution, as is typical of polymers. The inclusion of PC in the formulations had a synergistic effect, significantly increasing the extent of dissolution for all carriers, whereas only a minimal increase was observed when PC was added to crystalline RTV. AP and FR formulations with PC outperformed the commercial RTV formulations. The study also indicated that silicates, particularly AP and FR, preserved the amorphous nature of RTV during stability testing because the pore confinement of RTV prevented crystallization. The silicates also showed one important advantage over PVPVA; even at higher drug loading, the dissolution performance remained unaffected. Regression analysis of dissolution revealed that the major factors contributing to RTV dissolution were the presence of PC, AP, and FR, whereas BT and 'PVPVA × Drug load' interactions reduced dissolution. Thus, silicate carriers present a potential alternative to polymers for formulating solid dispersions. In silico investigations revealed that the pore size of the silicate carrier likely influenced the release performance of RTV. MD simulations in the open silica pore resulted, on average, in fewer hydrogen bonds than in the closed pore systems, as well as in a systematic exit of the RTV from the pore. These observations were consistent with the experimentally measured dissolution enhancement of RTV when loaded on AP.

CRediT authorship contribution statement

Gaurav Dhumal: Writing – review & editing, Writing – original draft, Methodology, Investigation, Conceptualization. **Adélaïde Savoy:** Writing – review & editing, Writing – original draft, Methodology, Investigation, Conceptualization. **Martin Kuentz:** Writing – review & editing, Conceptualization. **James E. Polli:** Conceptualization, Funding acquisition, Supervision, Validation, Writing – review & editing.

Declaration of competing interest

The authors declare that they have no known competing financial interests or personal relationships that could have appeared to influence the work reported in this paper.

Acknowledgement

This work was funded by the University of Maryland Strategic Partnership: MPowering the State (MPower).

Appendix A. Supplementary material

Supplementary data to this article can be found online at https://doi.org/10.1016/j.ijpharm.2026.127399.

Data availability

Data will be made available on request.

References

Baek, M.J., Kim, G.H., Park, J.H., Kim, J., Kang, I.M., Lee, J.I., Kim, D.D., 2022. Effect of phosphatidylcholine in bentonite-quetiapine complex on enhancing drug release and oral bioavailability. Int. J. Pharm. 628. https://doi.org/10.1016/j.ijpharm.2022.122347.

Baek, M.J., Park, J.H., Nguyen, D.T., Kim, D., Kim, J., Kang, I.M., Kim, D.D., 2023. Bentonite as a water-insoluble amorphous solid dispersion matrix for enhancing oral bioavailability of poorly water-soluble drugs. J. Control. Release 363, 525–535. https://doi.org/10.1016/j.jconrel.2023.09.051.

Bhujbal, S.V., Mitra, B., Jain, U., Gong, Y., Agrawal, A., Karki, S., Taylor, L.S., Kumar, S., Tony Zhou, Q., 2021. Pharmaceutical amorphous solid dispersion: a review of manufacturing strategies. Acta Pharm. Sin. B 11, 2505. https://doi.org/10.1016/J.APSB.2021.05.014.

Bukara, K., Schueller, L., Rosier, J., Martens, M.A., Daems, T., Verheyden, L., Eelen, S., Van Speybroeck, M., Libanati, C., Martens, J.A., Van Den Mooter, G., Frérart, F., Jolling, K., De Gieter, M., Bugarski, B., Kiekens, F., 2016. Ordered mesoporous silica to enhance the bioavailability of poorly water-soluble drugs: proof of concept in man. Eur. J. Pharm. Biopharm. 108, 220–225. https://doi.org/10.1016/j.ejpb.2016.08.020.

Coutinho, A.L., Adhikari, A., Krug, S., Kane, M., Hollenbeck, R.G., Hoag, S.W., Polli, J.E., 2025. In vitro-in vivo correlation of amorphous solid dispersion enabled itraconazole tablets. Pharm. Res. 42, 485–502. https://doi.org/10.1007/s11095-025-03837-z.

Dening, T.J., Taylor, L.S., 2018. Supersaturation potential of ordered mesoporous silica delivery systems. Part 1: dissolution performance and drug membrane transport rates. Mol. Pharm. 15, 3489–3501. https://doi.org/10.1021/acs.molpharmaceut.8b00488.

Dhumal, G., Treffer, D., Polli, J.E., 2024. Concordance of vacuum compression molding with spray drying in screening of amorphous solid dispersions of itraconazole. Int. J. Pharm. 654. https://doi.org/10.1016/j.ijpharm.2024.123952.

Ditzinger, F., Price, D.J., Nair, A., Becker-Baldus, J., Glaubitz, C., Dressman, J.B., Saal, C., Kuentz, M., 2019. Opportunities for successful stabilization of poor glass-forming drugs: a stability-based comparison of mesoporous silica versus hot melt extrusion technologies. Pharmaceutics 11, 577. https://doi.org/10.3390/pharmaceutics11110577.

Ellenberger, D.J., Miller, D.A., Kucera, S.U., Williams, R.O., 2018. Generation of a weakly acidic amorphous solid dispersion of the weak base ritonavir with equivalent in vitro and in vivo performance to Norvir tablet. AAPS PharmSciTech 19, 1985–1997. https://doi.org/10.1208/s12249-018-1060-x.

Heikkilä, T., Salonen, J., Tuura, J., Kumar, N., Salmi, T., Murzin, D.Y., Hamdy, M.S., Mul, G., Laitinen, L., Kaukonen, A.M., Hirvonen, J., Lehto, V.P., 2007. Evaluation of mesoporous TCPSi, MCM-41, SBA-15, and TUD-1 materials as API carriers for oral drug delivery. Drug Deliv. 14, 337–347. https://doi.org/10.1080/10717540601098823.

Jo, K., Cho, J.M., Lee, H., Kim, E.K., Kim, H.C., Kim, H., Lee, J., 2019. Enhancement of aqueous solubility and dissolution of celecoxib through phosphatidylcholine-based dispersion systems solidified with adsorbent carriers. Pharmaceutics 11. https://doi.org/10.3390/pharmaceutics11010001.

Kraus, H., Rybka, J., Höltzel, A., Trebel, N., Tallarek, U., Hansen, N., 2021. PoreMS: a software tool for generating silica pore models with user-defined surface functionalisation and pore dimensions. Mol. Simul. 47, 306–316. https://doi.org/10.1080/08927022.2020.1871478.

Li, J., Wang, X., Zhang, T., Wang, C., Huang, Z., Luo, X., Deng, Y., 2015. A review on phospholipids and their main applications in drug delivery systems. Asian J. Pharm. Sci. https://doi.org/10.1016/j.ajps.2014.09.004.

Li, J., Wang, Y., Yu, D., 2023. Effects of additives on the physical stability and dissolution of polymeric amorphous solid dispersions: a review. AAPS PharmSciTech 24. https://doi.org/10.1208/s12249-023-02622-8.

Liu, X., Lu, X., Su, Y., Kun, E., Zhang, F., 2020. Clay-polymer nanocomposites prepared by reactive melt extrusion for sustained drug release. Pharmaceutics 12. https://doi.org/10.3390/pharmaceutics12010051.

Liu, H., Scott, H.M., Lin, B., Huang, X., Smith, M.D., Shimizu, K.D., 2025. Solvent attenuation of dispersion interactions quantified in polar and nonpolar media using rigid ch–π balances. Chem. Sci. 16, 17772–17778. https://doi.org/10.1039/d5sc02852c.

Lu, C., Wu, C., Ghoreishi, D., Chen, W., Wang, L., Damm, W., Ross, G.A., Dahlgren, M.K., Russell, E., Von Bargen, C.D., Abel, R., Friesner, R.A., Harder, E.D., 2021. Opls4: improving force field accuracy on challenging regimes of chemical space. J. Chem. Theory Comput. 17, 4291–4300. https://doi.org/10.1021/acs.jctc.1c00302.

Men, S., Polli, J.E., 2024. Microscope-enabled disc dissolution system: concordance between drug and polymer dissolution from an amorphous solid dispersion disc and visual disc degradation. J. Pharm. Sci. 113, 3586–3598. https://doi.org/10.1016/j.xphs.2024.10.039.

Mohamadi, F., Richards, N.G., Guida, W.C., Liskamp, R., Lipton, M., Caufield, C., Chang, G., Hendrickson, T., Still, W.C., 1990. Macromodel—an integrated software system for modeling organic and bioorganic molecules using molecular mechanics. J. Comput. Chem. 11, 440–467. https://doi.org/10.1002/jcc.540110405.

Pollice, R., Bot, M., Kobylianskii, I.J., Shenderovich, I., Chen, P., 2017. Attenuation of London dispersion in dichloromethane solutions. J. Am. Chem. Soc. 139, 13126–13140. https://doi.org/10.1021/jacs.7b06997.

Roger, E., Lagarce, F., Benoit, J.P., 2009. The gastrointestinal stability of lipid nanocapsules. Int. J. Pharm. 379, 260–265. https://doi.org/10.1016/j.ijpharm.2009.05.069.

Shah, D.D., Taylor, L.S., 2024. Chemistry and ionization of HPMCAS influences the dissolution and solution-mediated crystallization of posaconazole amorphous solid dispersions. J. Pharm. Sci. https://doi.org/10.1016/j.xphs.2024.08.023.

Shen, Z., Simon, G.P., Cheng, Y.-B., 2002. Comparison of Solution Intercalation and Melt Intercalation of Polymer-Clay Nanocomposites.

Skrdla, P.J., Coscia, B.J., Gavartin, J., Browning, A., Shelley, J., 2023. Drug aggregation of sparingly-soluble ionizable drugs: molecular dynamics simulations of papaverine and prostaglandin F2A. Mol. Pharm. 20, 5135–5147. https://doi.org/10.1021/acs.molpharmaceut.3c00429.

Van Speybroeck, M., Mellaerts, R., Mols, R., Thi, T.D., Martens, J.A., Van Humbeeck, J., Annaert, P., Van den Mooter, G., Augustijns, P., 2010a. Enhanced absorption of the poorly soluble drug fenofibrate by tuning its release rate from ordered mesoporous silica. Eur. J. Pharm. Sci. 41, 623–630. https://doi.org/10.1016/j.ejps.2010.09.002.

Van Speybroeck, M., Mols, R., Mellaerts, R., Thi, T.D., Martens, J.A., Humbeeck, J.V., Annaert, P., Mooterden, G.V., Augustijns, P., 2010b. Combined use of ordered mesoporous silica and precipitation inhibitors for improved oral absorption of the poorly soluble weak base itraconazole. Eur. J. Pharm. Biopharm. 75, 354–365. https://doi.org/10.1016/j.ejpb.2010.04.009.

Vraníková, B., Niederquell, A., Šklubalová, Z., Kuentz, M., 2020. Relevance of the theoretical critical pore radius in mesoporous silica for fast crystallizing drugs. Int. J. Pharm. 591, 120019. https://doi.org/10.1016/j.ijpharm.2020.120019.

Xu, H., Krakow, S., Shi, Y., Rosenberg, J., Gao, P., 2018. In vitro characterization of ritonavir formulations and correlation to in vivo performance in dogs. Eur. J. Pharm. Sci. 115, 286–295. https://doi.org/10.1016/j.ejps.2018.01.026.

Yeo, S., An, J., Park, C., Kim, D., Lee, J., 2020. Design and characterization of phosphatidylcholine-based solid dispersions of aprepitant for enhanced solubility and dissolution. Pharmaceutics 12. https://doi.org/10.3390/pharmaceutics12050407.